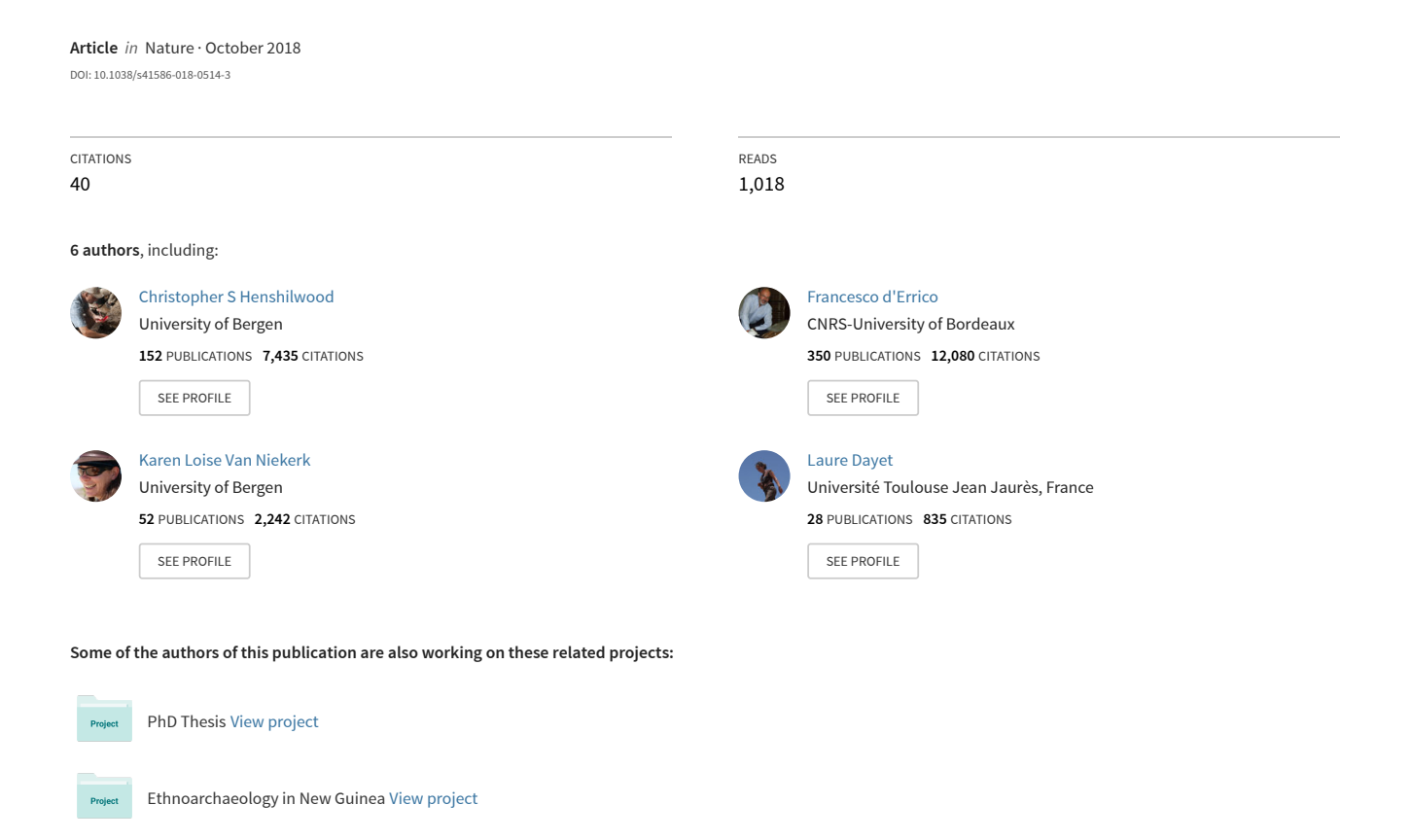
### An abstract drawing from the 73,000-year-old levels at Blombos Cave, South Africa





#### SUPPLEMENTARY INFORMATION

https://doi.org/10.1038/s41586-018-0514-3

In the format provided by the authors and unedited.

### An abstract drawing from the 73,000-year-old levels at Blombos Cave, South Africa

Christopher S. Henshilwood<sup>1,2</sup>\*, Francesco d'Errico<sup>1,3</sup>, Karen L. van Niekerk<sup>1</sup>, Laure Dayet<sup>3,4</sup>, Alain Queffelec<sup>3</sup> & Luca Pollarolo<sup>5,6</sup>

<sup>1</sup>SFF Centre for Early Sapiens Behaviour (SapienCE), University of Bergen, Bergen, Norway. <sup>2</sup>Evolutionary Studies Institute, University of the Witwatersrand, Johannesburg, South Africa. <sup>3</sup>CNRS UMR 5199, University of Bordeaux, Bordeaux, France. <sup>4</sup>Laboratoire TRACES UMR 5608, Université Toulouse Jean Jaures, Toulouse, France. <sup>5</sup>Unité d'Anthropologie/Laboratoire Archéologie et Peuplement de l'Afrique, Geneva, Switzerland. <sup>6</sup>School of Geography, Archaeology and Environmental Studies, University of the Witwatersrand, Johannesburg, South Africa. \*e-mail: christopher. henshilwood@uib.no

## An abstract drawing from the 73,000 year old levels at Blombos Cave, South Africa

#### Christopher S. Henshilwood, Francesco d'Errico, Karen L. van Niekerk,

#### Laure Dayet, Alain Queffelec and Luca Pollarolo

#### **Supplementary Information**

#### **Supplementary Discussion**

<ul> <li>Microscopic examinat</li> </ul>	ion and chemical analyses	Page 2
• Experimental marking	g of silcrete flakes	Page 4
• Ochre deposits from h	ammer-stone contact	Page 5
• Tribological analysis		Page 6
• References		Page 7
<b>Supplementary Tables</b>		
• SI Table 1		Page 8
• SI Table 2		Page 8
• SI Table 3		Page 9

#### Microscopic examination and chemical analyses

The red lines on L13 consist of juxtaposed patches of red deposits. The deposits accumulated in micro-concavities are composed of fine-grained bright red particles. Deposits on flat areas form a thin compact layer and are darker in colour. The latter are frequently associated with parallel striations oriented along the direction of the line (Main text Fig. 4).

The red material consists mainly of fine grained iron oxide (Fe) (Extended data Fig. 1a-b, SI Table 2). Variable contents of Si, associated with Fe, may come from the silcrete beneath the patches. Traces of Ti in line 5 are probably part of the iron-rich material of this line. Ti is seldom detected in the silcrete of L13 but, when present, does not show the same systematic association recorded on the red patches. The two small red deposits on the flake scar adjacent to the marked surface also consist mainly of Fe (SI Table 2). Haematite is identified by Raman within the red line deposits analysed (Extended data Fig. 1c). Quartz is sometimes present but, as the red deposits are thin, the detected quartz may be a component of the silcrete rather than the red patches. Iron-rich deposits are only associated with the patches composing the lines, indicating that there is no haematite in the L13 silcrete.

The surface of the silcrete with the drawing is smoothed (see below, Tribological Analysis). The quartz grains are flattened and some of the larger grains show micro-pitting associated, in some cases, with incipient fractures (Extended data Fig. 2a). A few areas show microstriations that cross both the matrix and the quartz grain. Micro-residues of red powder occasionally occur within depressions in the matrix and the micro-pits. These residues are mainly composed of particles rich in iron oxide (Fe) (Extended Data Fig. 2, SI Table 2). Haematite has been identified in all micro-residues analysed (Extended data Fig. 2c). The significant concentration of Si detected by SEM-EDS and the quartz signal on the Raman spectra are likely due to the underlying quartz grains. The Fe content of the micro-residues is substantially higher than that of the natural silcrete, but lower than in the red lines (see SI Table 2).

Silcrete is generally composed of quartz grains surrounded by a matrix of micro- to crypto-crystalline silica with the possible presence of other minerals<sup>1,2</sup>. On the drawn face of L13 quartz grains are relatively large and densely distributed within the matrix. Most are translucent but several are dark,

often black in colour. SEM-EDS and Raman analyses confirm that these dark grains are quartz.

Grains of zircon (Zr, Si) are also identified. The matrix of L13 comprises silica (Si), possible clay minerals (Si, Al), calcite (Ca, C), and iron oxide (Fe) (SI Table 2). Some of these elements may derive from the sediment in which L13 was deposited. The carbon detected on the surface could be from a thin calcite layer or indicate an organic coating.

To clarify the composition of the silcrete and the taphonomic history of L13, further analyses were done on the dorsal surface of L13, opposite to the drawn surface. This face is composed of silica grains (Si) and the matrix is rich in Si (SI Table 2). As Ca and C are the two most dominant elements after Si, it is likely that a thin layer of calcite is present on this surface, similar to that seen on the drawn surface. Significantly, the Fe concentration is very low on this face compared to that in the red lines and the micro-residues in-between the quartz grains on the drawn surface (SI Table 2). Orange spots, visible under the microscope, are not detected with SEM back-scattered electron imagery indicating the absence of heavy elements such as Fe. There is an unusual presence of Ti and Fe in one of the spots analysed (SI Table 2), which may derive from the surrounding sediment.

The chemical composition and microscopic analysis of the red lines on L13, indicates that ochre was applied to the surface. Experimental reproduction of these lines on silcrete flakes using two techniques (See above, Methods, SI Table 1 and Extended data figs. 3) indicate that they were produced by marking the surface with the edge of a thin ochre piece. The microscopic deposits of iron oxide rich particles detected on the drawn surface outside of the lines, and found only on this surface, are anthropogenic. They are mainly located on the smoothest areas, and are associated with micro-pits on quartz grains and striations identified by confocal microscopy. They are likely due to grinding ochre on this surface prior to the application of the red lines. The faint nature of these deposits suggests that the surface was cleaned, removing most of the ochre, before the lines were drawn. The red deposit on the flake scar, adjacent to the smoothed surface of L13, may result from unsuccessful attempts to produce a line on this rough surface.

Elemental composition of the different items analysed: the particles composing the red powder of the lines; the particles of the red micro-agglomerates; the grains and the matrix of the silcrete. Semi-

quantitative data have been used to range each element (weight percentages normalized to 100%, with C and O included).

#### **Experimental marking of silcrete flakes**

Tracing a line of red paint with a thin wooden brush on a flat silcrete surface produces an elongated stripe entirely covered by paint with well-defined edges (Extended Data Fig. 3a). The application of a thin paint results in a homogenous layer (Extended Data Fig. 3a[a and d]) whereas with medium density paint the edges of the line become more irregular, the mixture accumulates in concave areas and displays cracks after drying (Extended Data Fig. 3a[b and e]). Thick paint produces a discontinuous line with accumulations of paint in places along the line edges (Extended Data Fig. 3a[c and f]). As with the medium density paint, numerous cracks appear after drying. In all three cases, although rinsing under running water removes the accumulations of dried paint, the painted surface remains homogeneously covered by ochre residues and the painted and non-painted surfaces remain clearly distinguishable (Extended Data Fig. 3a[g-i]). With thick paint, the edges of the line are marked by a thin continuous boundary (Extended Data Fig. 3a[i]). Lines made by a single stroke of an ochre crayon (with a pointed or linear edge) on a silcrete surface result in discontinuous patches of ochre with irregular outlines (Extended Data Fig. 3b, SI Table 1). In some patches there are two distinct areas: a recess, partially filled with ochre powder, followed by a flat area covered by a deposit of ochre with parallel striations (Extended Data Fig. 3b[b and c]). The relative location of these two areas indicates the direction of the movement of the ochre crayon while producing the line. The shaving effect of micro-protrusions on the silcrete produces powder that accumulates in recesses. The pressure then produces a compacted streak of ochre on the following raised surface. Striations on this coating are produced by abrasive particles present in the ochre. Oneor multiple- strokes only leaves a minute amount of loose ochre powder on the silcrete flake. Cleaning the silcrete flakes marked with a crayon by rinsing with water removes the excess loose powder, leaving the compacted ochre lines in situ (Extended Data Fig. 3b [h and i]). Striations on the lines are still visible. Superimposing a line on a previous line generally results in a wider line as it is difficult to exactly superimpose a new line on the previous one. Unidirectional, superimposed lines

retain the same features observed on a single stroke line. Multiple lines produced by a to-and-fro movement of the ochre edge show microscopic evidence that the crayon was moved in both directions (Extended Data Fig. 4).

Experimental marking of silcrete flakes with a variety of ochre crayons demonstrates that the morphology of lines will depend on the properties and composition of the ochre, the roughness of the silcrete surface, the pressure exerted, and the morphology of the ochre area in contact with the silcrete. In general, soft, plastic, clayish ochre will produce thicker, more continuous lines than silty or sand-rich ochre. Lines on fine grained silcrete will be better defined than on coarse silcrete. Stronger pressure will produce comparatively wider, thicker and better defined lines. Six lines made with each of eight unmodified ochre crayons had a maximum width ranging from c. 0.9 to 3.3 mm. When produced with a pointed ochre crayon the lines tend to be wider and more variable in width than those made with a linear edge (Extended Data fig. 5). The width of the latter is strongly correlated to the maximum width of the facets on the ochre piece. In contrast, no correlation is observed between the lines made with pointed crayons and the maximum width of the facets on the crayon. The width of the lines on the drawn cross-hatching present on L13 is comparable with that of the experimental lines. Its range (1.8 -2.9 mm) best fits the width variability observed when marking the silcrete with a pointed crayon rather than an edge. It indicates that a pointed ochre crayon was used to produce the cross hatching and that the facet of the crayon in contact with the silcrete was c. 1.3-2.9 mm wide.

#### Ochre deposits on striking platforms resulting from hammer-stone contact

We considered the possibility that the L13 drawing could result from ochre deposits left by an ochre or ochre-laden hammer-stone when the L13 flake was struck. Soriano *et al.*<sup>3</sup> record ochre residues on struck flakes recovered from the Still Bay (c.71 ka) levels at Sibudu Shelter. In their Plate 1 (pp.54) these flakes are clearly illustrated and the ochre splodges on the struck surfaces bear no resemblance to the pattern on L13. Soriano *et al.*<sup>3</sup> consider several ways in which ochre could have been deposited on the Sibudu flakes and favour the hypothesis of a direct utilization of ochre nodules as hammers. During our ongoing but unpublished lithic analysis of flakes from the Still Bay levels at Blombos Cave (c. 75-72 ka) we also note ochre traces on some platforms resembling those illustrated from

Sibudu. None of the ochre traces on these Blombos flakes bear any resemblance to the deliberate pattern on L13. As is the case for Sibudu, we have not recovered ochre hammer-stones in the Still Bay levels at Blombos Cave.

Even if ochre hammer-stones were used at Sibudu or Blombos Cave in the Still Bay levels there can be no relationship between these hammer-stones and the ochre crayon used to draw the design on L13. The thickness of the lines on L13 is indicative of a thin and light ochre piece that is incompatible with being used as a hammer. Full support for this hypothesis is provided earlier in this paper where we describe, experimentally, how we reproduce these lines and how we are thus certain of the method of application and the size of the crayon – the hammer-stone application method is thus a null hypothesis.

#### Tribological analysis

3D rendering of microscopic areas of L13 and silcrete flakes from BBC identifies flattening of the drawn surface of L13 (Extended Data Fig. 6a[a]), dissolution of the matrix between quartz grains on the cortex of the BBC silcrete flakes (Extended Data Fig. 6a[d]) and an unworn appearance of the other surfaces of L13 (Extended Data Fig. 6a[b]) and the ventral aspect of the BBC silcrete flakes (Extended Data Fig. 6a[c]). The latter two display well-preserved quartz grains featuring typical conchoidal fractures and no traces of cement dissolution. Three roughness parameters were able to distinguish the four groups of surfaces: Sq (root-mean-square height), Sdr (developed interfacial area ratio), which respectively measure the overall roughness of the surface and its complexity, and Spc, which measures the mean form of the peaks (pointed vs rounded). Results indicate that the drawn surface of L13 is smoother than the other surfaces of this piece and the ventral and cortical surfaces of the BBC flakes (Extended Data Fig. 6a[e]). Higher Sq, Sdr, and Spc values, indicating increased surface roughness, were measured on cortical surfaces. Such high values are due to weathering which dissolves the matrix, thus exposing the quartz grains. A Kruskall-Wallis multiple comparison test demonstrates that Sq, Sdr and Spc on the drawn surface is significantly lower (p<0.01) than that measured on the remainder of the analysed surfaces of L13 (SI Table 3).

Areal fractal analysis confirms a clear difference in roughness between the drawn and other surfaces of L13, which is consistent with the interpretation of the wear on the former as produced by grinding activities prior to the drawing (Extended data Fig. 6b). It also reveals that the dorsal (Extended data Fig 6c[d]) and ventral (Extended data Fig. 6c[e]) surfaces of the flake are rougher than the flake scars on the drawn (Extended data Fig. 6c[b]) and ventral face (Extended data Fig. 6c[c]). This suggests that these surfaces had slightly different taphonomic histories.

#### References

- Blatt, H., Tracy, R. J. & Owens, B. Petrology-Igneous. *Sedimentary, and Metamorphic: WH Freeman &Co, New York*, 377-380 (1996).
- Nash, D. J. & Ullyott, J. S. in *Geochemical sediments and landscapes* Vol. Nash, D.J. & Ullyott, J.S., 2007. Silcrete, in . (eds) Geochemical Sediments & Landscapes. , pp.95-143. (eds D.J. Nash & S.J. McLaren) 95-148 (Wiley-Blackwell, 2007).
- Soriano, S., Villa, P. & Wadley, L. Ochre for the toolmaker: shaping the Still Bay points at Sibudu (KwaZulu-Natal, South Africa). *Journal of African Archaeology* **7**, 41-54 (2009).

Tables

SI Table 1 | Data on experimental ochre crayons and resulting lines.

Tip	active area morphology	lithic surface type	orientation of the tip	Crayon tip angle (°)	Width at 3 mm from the tip (mm)	Thickness at 3 mm from the tip (mm)	Number of lines	Mean length of the lines (mm)	Fracture of the crayon	Min width mean (mm)	SD	Max width mean (mm)	SD
1	pointed	debitage	parallel to the width	92	6.43	3.81	6	41.1	no	2,083	0,648	1,445	0,786
2	pointed	debitage	parallel to the width	71	6.72	6.01	6	45.5	no	1,908	0,077	1,178	0,091
3	pointed	debitage	perpendicular to the width	75	6.78	3.36	6	44.5	no	2,003	0,18	1,203	0,313
4	pointed	cortex	perpendicular to the width	75	7.45	2.98	6	45.5	no	2,632	0,627	1,343	0,192
5	linear	debitage	parallel to the width	145	10.53	2.25	6	34	no	1,167	0,139	0,948	0,06
6	linear	debitage	parallel to the width	170	17.68	3.13	6	39.5	no	1,725	0,215	1,325	0,297
7	linear	debitage	parallel to the width	180	13.33	2.93	6	44.3	no	1,828	0,283	1,457	0,133
8	linear	debitage	parallel to the width	160	9.15	3.71	6	40.2	no	1,985	0,338	1,282	0,209

SI Table 2 | Summary of the SEM-EDS analyses on the lines and other surfaces of L13.

Location of the analysis	Item analysed	Major elements	Minor elements	Minor to trace	Interpretation	
	(BSE contrast)	>10%	>3%	<3%		
Red line 5, Locus C	'Bright' fine particles	Fe, Si, C		Ca, Al, Ti, Na, Mg, P, K	Iron oxide particles +?	
	'Bright' fine particles	Fe, C	Si	Ca, Al, Ti, Na, Mg, P, K	Iron oxide particles +?	
	'Bright' fine particles	Fe, C	Si, Ca	Al, Ti, Na, Mg, P, K	Iron oxide particles +?	
	'Very bright' coarse grain	Zr, Si, C		Ca, Fe, Na, Mg, Ti	Zircon +?	
	'Grey' coarse grain	Si, C	Fe	Ca, Na, Al, P	Quartz grain +?	
	'Grey' matrix	Si, C	Al, Ca	Fe, Na, Mg, P	Silica +?	
Red line 5, Locus F	'Bright' fine particles	Fe, Si, C	Ca	Al, Ti, Na, Mg, P, K	Iron oxide particles +?	
	'Bright' fine particles	Fe, Si, C	Ca	Al, Ti, Na, Mg, P, K	Iron oxide particles +?	
Red line 2, Locus C	'Bright' fine particles	Fe	C, Si, Ca	Al, Ti, Na, Mg, P, K	Iron oxide particles +?	
	'Bright' fine particles	Fe	C, Si, Ca	Al, Ti, Na, Mg, P, K	Iron oxide particles +?	
	'Grey' coarse grain	Si, C	Fe	Ca, Al, Mg, P	Quartz grain +?	
Red line 6, Locus E	'Bright' fine particles	Fe	C, Si, Ca	Al, Ti, Na, Mg, P, K	Iron oxide particles +?	
	'Very bright silt grain	Zr, Si, C	Ca	Fe, Na, Mg, Ti	Zircon	
Red patch, Locus F	'Bright' fine particles	Fe	C, Si	Al, Ti, Na, Mg, P, K	Iron oxide particles +?	
Red micro-agglomerates, Locus E	'Grey' coarse grain	Si, C, Ca		Fe, Al, Mg, Na	Quartz grain +?	
	'Grey' coarse grain	Si, C	Ca, Fe	P, Na, Mg, Al	Quartz grain +?	
	'Bright' fine particles	Fe, Si, Ca, C		P, Na, Mg, Al, K	Iron oxide particles +?	
	'Bright' fine particles	Si, Fe, C	Ca	P, Na, Mg, Al, K	Silica + Iron oxide particles	
	'Grey' matrix	Si, Ca, C		Fe, P, Na, Mg, Al, K	Silica +?	
	'Grey' matrix	Ca, Si, C	Fe	P, Na, Mg, Al, K	Calcite +?	
Red micro-agglomerates, Locus F	'Grey' matrix	Ca, Si, P	C, Ca	Al, Na, Mg, P, K	Silica +?	
	'Bright' fine particles	Fe, Si	C	Al, Mn, Na, Mg, P, K	Iron oxide particles +?	
	'Bright' fine particles	Fe, Si	C	Al, Na, Mg, P, K	Iron oxide particles +?	
	'Grey' coarse grain	Si, C	Ca	Fe, Na, Mg, P	Quartz grain + ?	
Silcrete, Locus E	'Grey' matrix	Si, C		Ca	Silica +?	
	'Grey' matrix	Si, C	Ti, Fe	Ca, Mg, Al	Silica + ?	

# SI Table 3 | Kruskall-Wallis test of the difference between roughness variables measured on the drawn and other surfaces of BBC L13 and the knapped and cortical surfaces of two MSA silcrete flakes from BBC.

Kruskall-Wallis (Sq)	p = 5.946458e-23			
Comparison between groups	p < 0,05	p < 0,01		
BBC L13 - drawn surface vs. BBC L13 - other surfaces	TRUE	TRUE		
BBC L13 - drawn surface vs. BBC MSA flakes - knapped surfaces	TRUE	TRUE		
BBC L13 - drawn surface vs. BBC MSA flakes - cortical surfaces	TRUE	TRUE		
BBC L13 - other surfaces vs. BBC MSA flakes - knapped surfaces	TRUE	FALSE		
BBC L13 - other surfaces vs. BBC MSA flakes - cortical surfaces	TRUE	TRUE		
BBC MSA flakes - knapped surfaces vs. BBC MSA flakes - cortical surfaces	TRUE	TRUE		
Kruskall-Wallis (Sdr)	p = 3.207647e-22			
Comparison between groups	p < 0,05	p < 0,01		
BBC L13 - drawn surface vs. BBCL13 - other surfaces	TRUE	TRUE		
BBC L13 - drawn surface vs. BBC MSA flakes - knapped surfaces	FALSE	FALSE		
BBC L13 - drawn surface vs. BBC MSA flakes - cortical surfaces	TRUE	TRUE		
BBC L13 - other surfaces vs. BBC MSA flakes - knapped surfaces	TRUE	TRUE		
BBC L13 - other surfaces vs. BBC MSA flakes - cortical surfaces	TRUE	TRUE		
BBC MSA flakes - knapped surfaces vs. BBC MSA flakes - cortical surfaces	TRUE	TRUE		
Kruskall-Wallis (Spc)	p = 3.74638e-10			
Comparison between groups	p < 0,05	p < 0,01		
BBC L13 - drawn surface vs. BBCL13 - other surfaces	TRUE	TRUE		
BBC L13 - drawn surface vs. BBC MSA flakes - knapped surfaces	FALSE	FALSE		
BBC L13 - drawn surface vs. BBC MSA flakes - cortical surfaces	TRUE	TRUE		
BBC L13 - other surfaces vs. BBC MSA flakes - knapped surfaces	TRUE	TRUE		
BBC L13 - other surfaces vs. BBC MSA flakes - cortical surfaces	FALSE	FALSE		
BBC MSA flakes - knapped surfaces vs. BBC MSA flakes - cortical surfaces	TRUE	TRUE		